Importance of the electrode conductivity in organic photovoltaic solar cells

M. Hssein, [1,3]

L. Cattin, [1]

M. Morsli, [2]

M. Addou, [3]

J. C. Bernède, [4,*]

Email jean-christian.bernede@univ-nantes.fr

[1] Institut des Matériaux Jean Rouxel (IMN), CNRS, UMR 6502, 2 rue de la Houssinière, BP 32229, 44322 Nantes Cedex 3, France

[2] Faculté des Sciences et des Techniques, 2 rue de la Houssinière, BP 32229, 44322 Nantes Cedex 3, France

[3] LMVR, FST, Université Abdelmalek Essaidi, Tanger, Ancienne Route de l'Aéroport, Km 10, Ziaten, BP 416, Tétouan, Morocco

[4] MOLTECH-Anjou, CNRS, UMR 6200, 2 rue de la Houssinière, BP 92208, 44000 Nantes, France

Abstract

Realization of performing large area flexible organic photovoltaic cells needs highly conductive and transparent electrode. In the present manuscript we show that it is possible to improve the power conversion efficiency of organic solar cells deposited onto PET/ITO anode by improving the conductivity of the anode. When covered with a thin, 12 nm, metal bilayer, Cu/Ag, itself covered by a refractory metal oxide, MoO_3 or WO_3, it is possible to significantly decrease the sheet resistance of the ITO anode, while its transmission is only slightly reduced, which result in a

figure of merit as high as $32 \times 10^{-3}\ \Omega^{-1}$. Moreover, the flexibility of these multilayer structures is better than that of ITO alone. In the case of PET substrates, when these optimized anodes are introduced in photovoltaic cells based on the planar heterojunction CuPc/C_{60}, the power conversion efficiency of these cells is higher than that of the cells using ITO alone. This improvement becomes more significant and useful for larger areas devices that are needed for practical applications. The best results are obtained with ITO/Cu/Ag/WO_3 anodes.

AQ1

1. Introduction

During the last two decades, organic photovoltaic cells (OPVCs) have led to significant improvement in device performances [1, 2]. OPVCs with efficiencies above 10% have been demonstrated [3, 4]. OPVCs are based on an electron donor and an electron acceptor either blended in the form of a bulk-heterojunction (BHJ) or in the form of two superposed layers (planar heterojunction (PHJ) [5]. This device heart is sandwiched between two electrodes, one of them being transparent. A highly conductive and transparent electrode is of decisive importance for OPVCs because it significantly affects their efficiency. Up to now glass substrates are mainly used. However, demand for flexible components is growing steadily [6]. Currently, indium tin oxide (ITO) thin films are used as transparent electrode due to the high transparency and quite good conductivity of ITO. Therefore, usually OPVCs described in publications employ ITO as bottom electrode. Unfortunately, its application to large area devices is limited by its insufficient conductivity, mainly in the case of flexible substrates. Furthermore, ITO suffers from deterioration after repeated bending, which further decreases the conductivity. Therefore it is desirable to decrease the resistivity of the ITO electrode while increasing its flexibility. On the other hand, using dielectric/metal/dielectric (D/M/D) structures as possible transparent conductive electrode, we have shown that optimal optical transparency was obtained when we introduced a double metallic layer −Cu/Ag− between two ZnS films [7]. Actually, if D/M/D tri-layer structures exhibits very small sheet resistance, and a high maximum transmittance, the width of their transmission range is not as broad as that of TCOs. For instance, a typical example of D/M/D structure which performs well is given by NiO/Ag/NiO structures [8]. They exhibit an averaged transmission

between 400 and 700 nm of 79%, while that of ZnS/Cu/Ag/ZnS is 90% for the same transmission range [7], which justifies our choice. It can be noted that such widening effect due to the use of metal bilayer, Cu/Ag, was also demonstrated in the case of ultra-thin metal films [9]. However, the transmission is higher if the metal layers are inserted between two dielectric layers, thanks to the high refractive index of the dielectric used in these structures. For instance, at 420 nm, the refractive index of ITO is 2, while that of PET is 1.68, which allows increasing the transmission of the electrode by introducing an ITO layer between PET and metal layer.

Nevertheless, our attempts to use ZnS in optoelectronic devices were somewhat disappointing, due to poor carrier extraction properties of ZnS. Therefore in the present study, starting from commercial ITO deposited either on glass or on PET, we proceed to improve its electrical and mechanical properties through the use of a double metal layer, Cu/Ag, and a refractory metal oxide MoO_3 or WO_3. Using this improved flexible ITO in OPVCs, especially in the case of larger surfaces, significantly increases the device performances.

2. Experimental details

2.1. Multilayer structures realization and characterization

ITO on glass substrates was provided by SOLEMS, while that deposited onto PET flexible substrates was provided by Aldrich. In the case of glass/ITO electrodes the sheet resistance was 20 Ω/sq and the maximum transmittance was 96%, while those of PET/ITO were 100 Ω/sq and 93% respectively.

About the films added to ITO, the procedure was described in a precedent publication [7]. After scrubbing with soap, the ITO coated substrates were rinsed under running deionised water. Then the substrates were dried with air flow. Finally they were loaded in the vacuum chamber (10^{-3} Pa). The Cu/Ag/oxide (MoO_3 or WO_3) were deposited by simple sequential joule effect, sublimation for the oxide, or evaporation for the metals, Cu, Ag and Al. Actually, as we will see below, in some samples, an ultrathin Al layer was inserted between Ag and MoO_3. The different layers were successively deposited onto ITO at room temperature, using simple tungsten nacelles for the metals and molybdenum crucible for the oxide. The tungsten nacelles were loaded with Cu, Ag or Al wires, while the molybdenum crucible was loaded with MoO_3 or WO_3 powder. After calibration through the use of a scanning

electron microscope, the deposition rate and thickness were measured in situ with a quartz monitor, with the help of a rotating mask. The optimum thickness and deposition rates of the different thin films were established in preceding manuscripts: 3 nm, 0.07 nm/s and 9 nm, 0.4 nm/s for Cu and Ag respectively [7] while they were 35 nm and 0.08 nm/s for the oxide [10].

The different multilayer structures used during this work were ITO, ITO/Cu /Ag/MoO_3, ITO/Cu/Ag/Al/$Mo0_3$ and ITO/Cu/Ag/$W0_3$, for simplicity, in the following text, they will be called ITO, ITOCAM, ITOCAAM and ITOCAW respectively.

The optical measurements were carried out at room temperature using a Perkin spectrophotometer. The optical transmission was measured in the 0.3–1.2 μm spectral range. The four-probe technique was used to measure the electrical conductivity. In order to measure the real potentialities of the different structures we use the classification technique proposed by Haacke [11]. The Figure of merit Φ_M proposed by Haacke is $\Phi_M = T^{10}/Rsq$, with T transmission and Rsq the sheet resistance of the structure.

The surface topography of the structures was observed with a field emission scanning electron microscope (SEM, JEOL F-7600). The SEM operating voltage was 5 kV.

The flexibility of the different anodes deposited onto PET was studied using a laboratory made bending system. The samples were clamped between two conductive parallel plates. The one was fixed to a mobile axis moved by the engine with back and, while the other one was fixed to a rigid support. The distance between the two plates in the stretched mode was 30 mm, while that of the bent position was 12 mm. The bending radius was approximated to 6 mm. During the bending test, the resistance of the sample was measured using an electrometer. The sample was loaded with the multilayer structure either facing upward (outer-bending) or downward (inner-bending).

2.2. Organic photovoltaic cells realization and characterization

In order to probe the multilayer electrodes, they were introduced in classical PHJ based on the couple CuPc/C_{60} sandwiched between two electrodes, the multilayer electrode ITO/Cu/Ag/oxide as anode and an Al film as cathode. Classical ITO anodes were also used as reference. Between the electrodes and

the organic materials buffer layers were inserted [5]. Between the Al cathode and the fullerene layer, the buffer layer, usually called exciton blocking layer (EBL), was Alq_3 [5]. The anode buffer layer (ABL) was a co-evaporated MoO_3:CuI hybrid layer. The deposition rate of the MoO_3 and CuI was 0.01 nm/s and the whole thickness of the ABL was 4.5 nm. CuI was coevaporated with MoO_3, since we have shown that such co-evaporated ABL allows combining the advantages of CuI and those of the transition metal oxide [12].

After the ABL, CuPc, C_{60}, Alq_3 were successively sublimated under vacuum and the aluminium anode was evaporated on the top of the device giving the following OPVC structure:

Anode/ABL/CuPc (35 nm)/C_{60} (40 nm)/Alq_3 (9 nm)/Al (120 nm). The anode is either one of the multilayer structures studied in the present work, or ITO. The top electrode was deposited through a mask with 2×8 mm^2 active area. All these thicknesses were optimized in previous publication [13]. The substrate was either glass or PET.

Electrical characterizations were performed with an automated I–V tester, in the dark and under AM 1.5 G simulated solar illumination. Performances of photovoltaic cells were measured using a calibrated solar simulator (Oriel 300 W) at 100 mW/cm^2 light intensity adjusted with a PV reference cell (0.5 cm^2 CIGS solar cell, calibrated at NREL, USA). Measurements were performed in ambient atmosphere. All devices were illuminated through TCO electrodes. We estimated the values of the shunt resistance (Rsh) and the series resistance (Rs), in order to assess the effect of the different anodes on the values of Rsh and Rs. The values for Rs and Rsh were estimated from the slopes at the open circuit voltage and short circuit current points on the I–V curve.

For comparison, OPVCs with ITO alone and ITO/Cu/Ag/oxide were realized during the same deposition processes. In order to check the reproducibility of the results, successive (3–4) runs were done for each configuration, which corresponds to 9–12 OPVCs in the case of small area and 4 in the case of large area cells.

The efficiency of such devices has not been fully optimized compared to the best performing CuPc/C_{60} solar cells in the literature, but since OPCVs using ITO/Cu/Ag/oxide and reference ITO anodes were produced by the same

procedure, their relative enhancement can be attributed only to the effect of the improved anode.

3. Results

3.1. Electro-optical characterization of the anodes

Both glass and flexible PET substrates were used during the experiments. The Cu, Ag and oxide films thicknesses were selected from previous studies, 3 nm of Cu, 9 nm of Ag [7] and 35 nm of oxide [10]. As we will see, the best devices were obtained with ITOCAW. Therefore, we compare in Fig. 1a, the transmission of this electrode to that of ITO alone, the substrate being glass. The highest transmission obtained with ITOCAW is 86%, while that of ITO is 96%. At the same time it must be noted that the sheet resistance measured by the four-probe technique decreases from 20 Ω/sq for ITO to 6.8 Ω/sq with ITOCAW.

Fig. 1

Transmission spectra of **a** ITO and ITO/Cu/Ag/WO_3 onto glass substrate (**a**) and of ITO, ITO/Cu/Ag/MoO_3, ITO/Cu/Ag/Al/MoO_3 and ITO/Cu/Ag/WO_3 onto PET substrate (**b**)

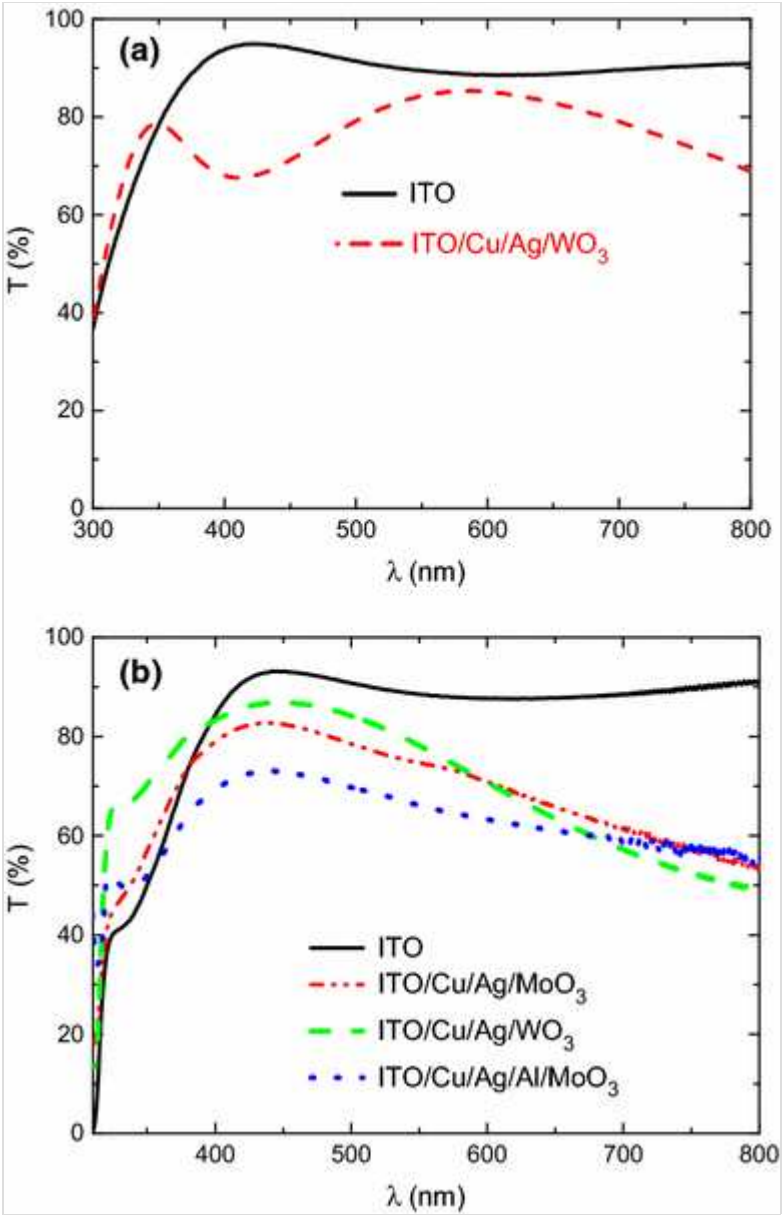

In order to compare the quality of these different electrodes we introduce the Figure of merit proposed by Haacke [11]. The Figure of merit calculated for the optimum structures presented above were $\Phi_M = 32.5 \times 10^{-3}\ \Omega^{-1}$ for ITOCAW and $\Phi_M = 9 \times 10^{-3}\ \Omega^{-1}$ for ITO alone. It means that modified ITO seems improved compared to ITO alone.

Similar study was conducted in the case of flexible PET substrate. The present study being more specifically dedicated to flexible substrates, we introduce also the results obtained with MoO_3, for comparison. In that case, due to the poor reproducibility of the cell performances, for some devices, an ultra thin Al film (about 1 nm) was introduced between Ag and MoO_3. The Fig. 1b shows that the highest transmission obtained with ITO is 94%, it is 87% with ITOCAW and 83% with ITOCAM, while it is only 73% when a thin Al film (1 nm) is inserted between Ag and MoO_3 (ITOCAAM). Such

unexpected large decrease of the transmission may be due to the uncertainty on the thickness value when such thin films are used (1 nm). Moreover this very thin Al film, which is probably oxidized, may take the form of agglomerates which can be a source of light scattering.

The sheet resistance measured for these electrodes were 100, 8.6, 15.6 and 9.6 Ω/sq for ITO, ITOCAW, ITOCAM and ITOCAAM respectively, which gives $\Phi_M = 5.4 \times 10^{-3}\ \Omega^{-1}$ for ITO, $\Phi_M = 28.8 \times 10^{-3}\ \Omega^{-1}$ for ITOCAW, $\Phi_M = 10 \times 10^{-3} \times \Omega^{-1}$ for ITOCAM and $\Phi_M = 4.5 \times 10^{-3}\ \Omega^{-1}$ for ITOCAAM. It means that the Figure of merit of ITOCAW is significantly improved compared with ITO alone. The differences in values obtained with the configurations containing MoO_3 will be discussed later. Since the modification of the ITO films, through the addition of Cu/Ag/oxide films, allows optimizing the electro-optical properties of the electrodes, we checked the mechanical properties of these different structures.

We measured the flexibility of the ITO/Metals/Oxide structures deposited onto PET substrates. The results are compared to commercial ITO onto PET where the sheet resistance is 100 Ω/sq. The change in resistance was expressed as $(R - R_0)/R_0$, where R_0 is the initial resistance and R the measured resistance after bending. The bending apparatus was designed to perform outer bending and inner bending tests. For outer bending measurements, the sample was loaded with the multilayer structure facing upward. For inner bending, the sample was loaded with the multilayer structure facing downward. The Fig. 2 shows the change in the resistance of the samples with increasing number of bending cycles. For all samples, the $(R - R_0)/R_0$ value increases quite quickly during the first 50 cycles and then it tends to stabilize. However, the relative resistance increase is far higher in the case of ITO alone. It means that ITO/Metals/Oxide structures exhibit smaller variation of their resistance value, indicating a better flexibility of these multilayer structures. Similar result is obtained for inner and outer bending tests. Th**e** good stability of the sheet resistance of the PET/Oxide /Ag/Oxide structures is usually attributed to the presence of the ductile Ag metal layer between both dielectric layers [14]. It can be noted that the presence of Al decreases the stability of the multilayer structure, while the best result is obtained when the oxide is WO_3.

Fig. 2

Flexibility of ITO, ITO/Cu/Ag/MoO_3, ITO/Cu/Ag/Al/MoO_3 and ITO/Cu /Ag/WO_3 onto PET, **a** outer bending, **b** inner bending

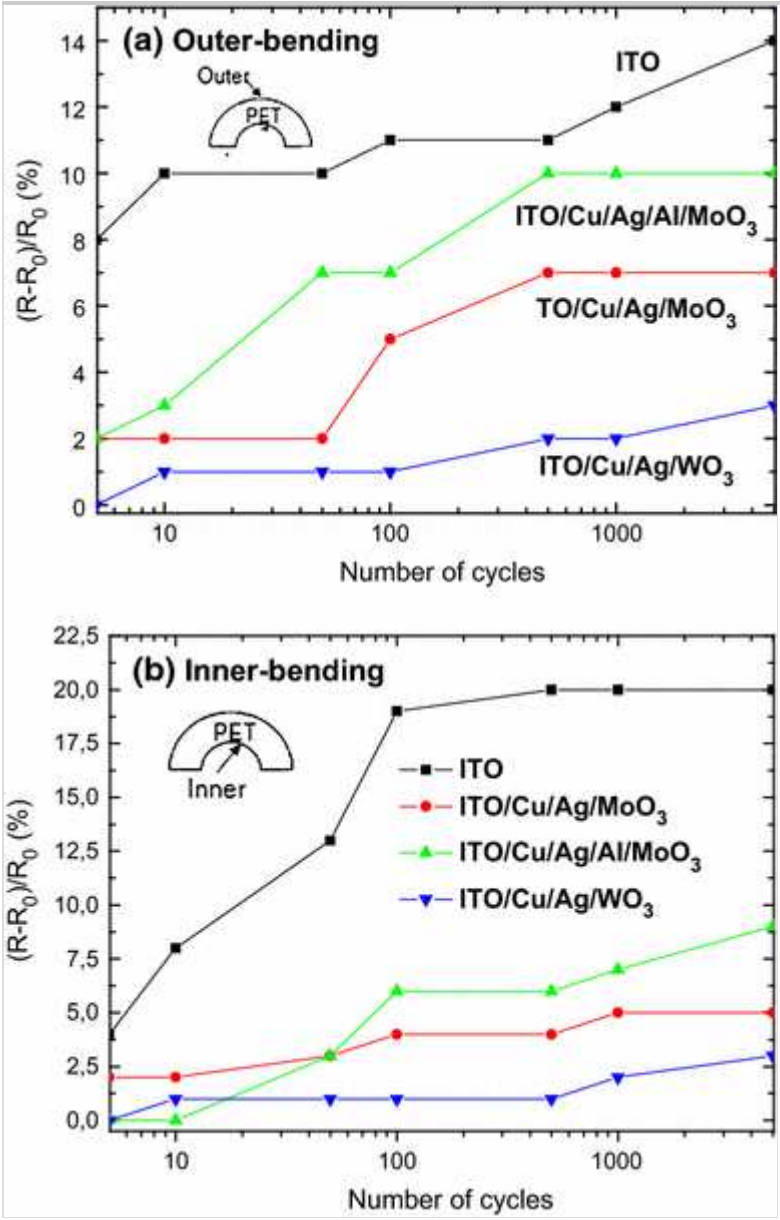

Figure 3a shows that the surface of the ITO films deposited onto PET is homogeneous and smooth with small grains regularly shaped. When covered with Cu/Ag/WO_3, the morphology of the films stays the same, the only difference being that the grains and grain boundaries are better visible in Fig. 3b. Actually, a statistical estimation of the grain diameter give roughly the same value, 25 nm, for both films.

Fig. 3

Surface visualization of ITO (**a**) and ITO/Cu/Ag/WO_3 (**b**) deposited onto PET substrate

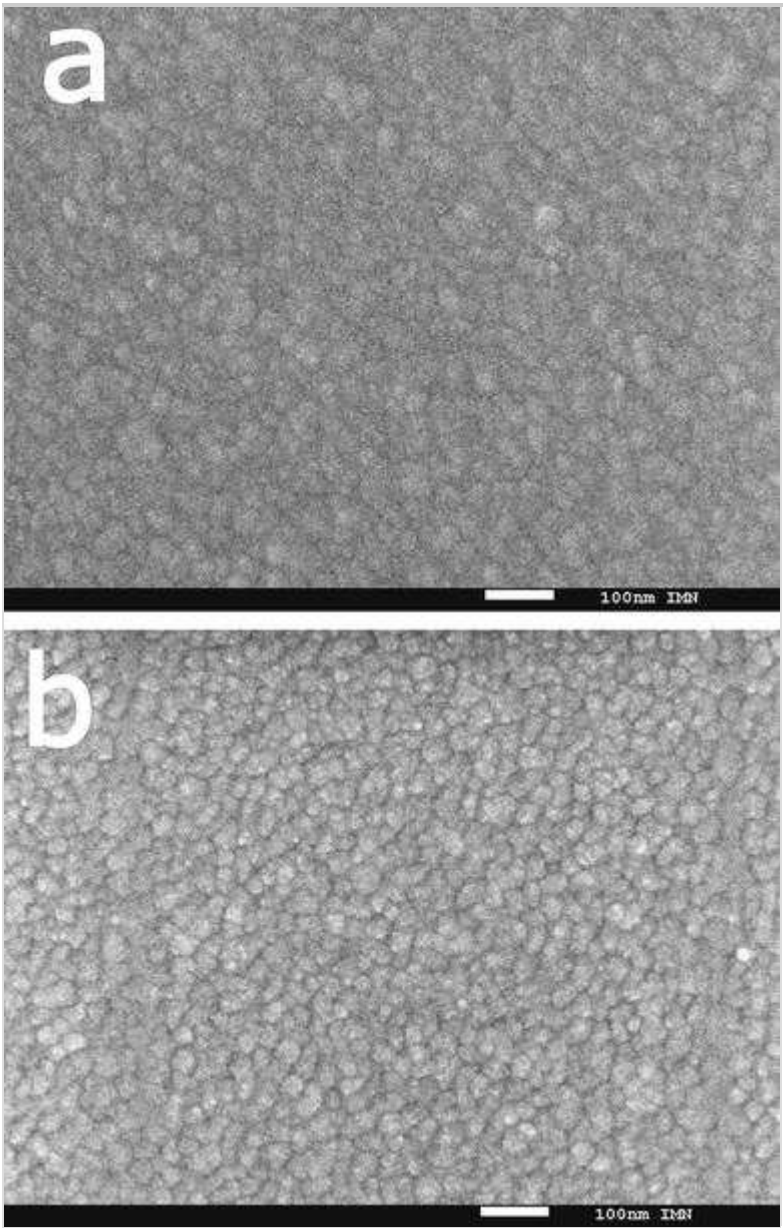

After characterization of the multilayer structures, in order to check their behaviour as electrodes, we used them as anode in OPVCs. We initially use glass substrates, even if the main goal of the present study is to improve the performance of flexible ITO. The results obtained with the two different oxides are presented in Table 1. It can be seen that the best performance is obtained with the classical ITO anode. It means that, for glass substrates, the active surface is small enough that the restriction of the device performance due to the sheet resistance value, which is low in the case of the glass substrate, is not perceptible. Actually, if, in the case of ITOCAW anode there

is a small increase of FF due to its highest conductivity, Jsc is smaller, due to its weaker transmission. About the devices with MoO_3 as top layer of the anode, it can be seen that it gives the worst results. The open circuit voltage Voc and fill factor FF are smaller than those of others electrode. These small values are due to a quite high leakage current. As a matter of fact, when MoO_3 is the top layer of the anode, there is systematically a high leakage current and the reproducibility of the results is poor. Sometimes, poor results are obtained due to very high leakage current. This difficulty encountered with MoO_3 will be discussed below. Nevertheless, this preliminary study shows the multilayer structure can be used as anode in OPVCs.

Table 1

Performances of OPVCs, deposited onto glass substrates with different anode configurations

Anode	Voc (V)	Jsc (mA/cm^2)	FF (%)	η (%)
ITO	0.47 ± 0.01	8.26 ± 0.10	46 ± 2	1.78 ± 0.15
ITOCAM[a]	0.43 ± 0.02	7.02 ± 0.15	44 ± 3	1.30 ± 0.30
ITOCAW	0.49 ± 0.01	6. 80 ± 0.10	48 ± 1	1.60 ± 0.10

[a]Due to the dispersion of the results obtained with ITO/Cu/Ag/MoO_3 anodes, see the manuscript, only OPVCs with efficiency higher than 1% has been taken into account

Typical J–V characteristics of flexible OPVCs are presented in Fig. 4, while averaged values are given Table 2. We introduce two series of results in the case of MoO_3. As a matter of fact, the reproducibility of the results is so bad that it is not possible to give averaged values which make sense, as the results vary widely from one sample to another one. It can be seen in the inset of Fig. 4 that, even in the case of the good sample presented (sample 1 of Table 2), the dark current is not negligible, which justifies the small Voc and FF. In Table 2 we see that the shunt resistance, Rsh, of the devices with MoO_3 is quite small. So, the leakage current is systematically not negligible and it varies strongly from one sample to another one, which justifies the wide dispersion of results. This disappointing result can be explained as follow. In the ITOCAM structures, under the Ag layer, there is a thin Cu layer. The Ag layer being thick of only 9 nm, it is probable that in some small areas, Cu is in direct contact with MoO_3. We have already shown that Cu diffuses spontaneously into MoO_3 [15], which might have induced the leakage

currents encountered. In order to try to overpass this difficulty, we introduced an ultrathin Al film (1 nm). We have shown in ref 15 that such Al layer, at least partially, prevents Cu diffusion into MoO_3. It must be noted that this Cu diffusion and the barrier diffusion effect of Al is corroborated by the sheet resistances of these electrodes, without Al, the sheet resistance of ITOCAM is 15.6 Ω/sq, due to Cu diffusion, while with Al the sheet resistance of ITOCAAM is only 9.6 Ω/sq. The results obtained with ITOCAAM are presented in Fig. 4 and Table 2. It is clear that the leakage current has significantly decreased, due to the increase of Rsh, which results in an increase of Voc and FF. However Jsc has strongly decreased and the efficiency of the OPVC is far smaller than that of the device using ITO alone as anode. This decrease must be related to the small transmission of the ITOCAAM electrode. Therefore we used another oxide. If MoO_3 is often used as anode buffer layer due to its high effectiveness, WO_3 has also been used with success. Recently it was shown that WO_3 allows growing more stable OPVCs than with MoO_3 [16]. Therefore, in order to improve the reproducibility of the results, we probe the structure ITOCAW, as transparent electrode in OPVCs. Here, for plastic substrates, the hierarchy is reversed. Even for a small active area, the ITO sheet resistance (100 Ω/sq) is such that the best results are obtained with ITOCAW anodes with sheet resistance of only 7.6 Ω/sq. It can be seen in Table 2 that, if, here also, Jsc is higher in the case of ITO, the increase of the others parameters, Voc, FF, is sufficient to induce an improvement of the efficiency of the OPVC with ITOCAW as anode. This improvement is clearly related to the large decrease of the series resistance, which is decreased by a factor of three. This result testifies that the limited conductivity of the ITO can be a limitation in the case of larger surface devices. That's why we tested cells whose surface area was 1 cm^2. The results obtained are presented in Fig. 5. It can be seen that the effect of the smaller sheet resistance of the ITOCAW anode is amplified, the power conversion efficiency of the OPVCs using this anode being 34% higher than that obtained with ITO alone. A similar result was obtained by T. Winkler et al., but in the case of inverted OPVCs, an electrode ZnO/Ag/ZnO was used as top electrode [17]. This result confirms that, in the case of large area, the sheet resistance of the electrodes is essential.

Fig. 4

J–V characteristics of OPVCs with different anodes, onto PET substrates, *full symbols* in the *dark* and *open symbols* under AM1.5 irradiation. *Inset*: *dark* currents for different anodes: (*filled square*) ITO and ITO/Cu/MoO_3/X with X = (*filled triangle*) MoO_3, (*filled inverted triangle*) Al/MoO_3, (*filled circle*)

WO_3

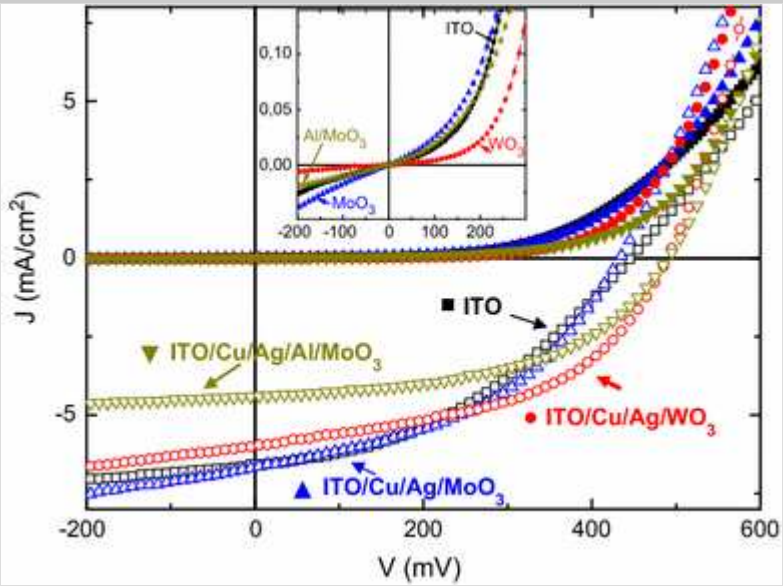

Table 2

Performances of OPVCs, deposited onto PET substrates with different anode configurations

Anode	Voc (V)	Jsc (mA/cm^2)	FF (%)	η (%)	Rs (Ω)	Rsh (Ω)
ITO	0.45 ± 0.01	6.50 ± 0.20	40 ± 1	1.17 ± 0.20	13 ± 2	285 ± 20
ITOCAM (1)	0.43[a]	6.53[a]	44[a]	1.27[a]	6[a]	175[a]
ITOCAM (2)	0.38[a]	6.19[a]	38[a]	0.90[a]	8[a]	110[a]
ITOCAAM	0.49 ± 0.02	4.52 ± 0.15	49 ± 2	1.08 ± 0.25	10 ± 2	850 ± 25
ITOCAW	0.49 ± 0.01	6.08 ± 0.15	50 ± 1	1.51 ± 0.15	4.5 ± 1.5	230 ± 15

[a]As discussed in the manuscript, the reproducibility of the results is so bad with the ITO/Cu/Ag/MoO_3 anodes that it is not possible to give averaged values which make sense

Fig. 5

J–V characteristics of OPVCs having 1 cm^2 of surface area, with different anodes. *Full symbols* in the *dark* and *open symbols* under AM1.5 irradiation. *Inset*: details about *dark* currents

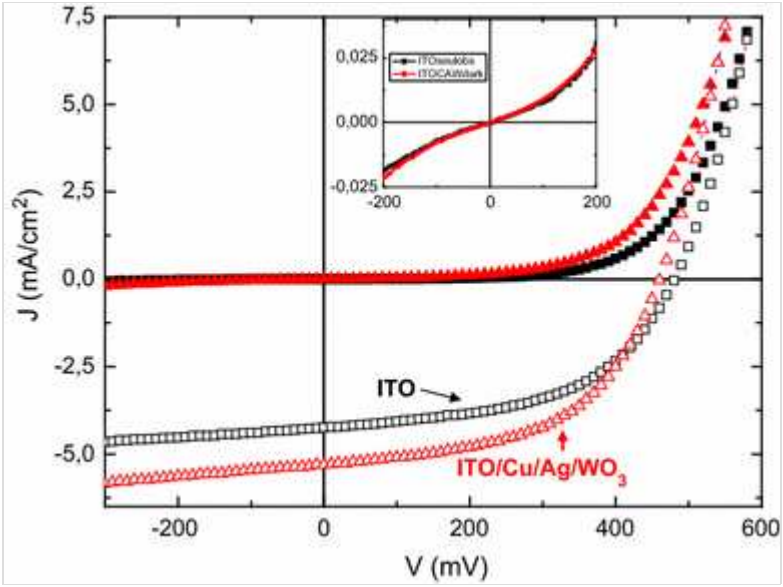

AQ2

Another positive effect expected of the covering of the ITO by $Cu/Ag/WO_3$ is improved flexibility of cells. It can be seen in Fig. 6 that, that the normalized efficiency of both OPVC families decreases, mainly during the first bending cycles. A similar trend is observed in the case of the resistance which seems to decrease. Nevertheless, as well as for the sheet resistance, the degradation is far higher in the case of classical ITO. Here, as said above, the ductile metal prevents failure formation.

Fig. 6

Relative variation of the OPVCs efficiency when they are submitted to bending tests

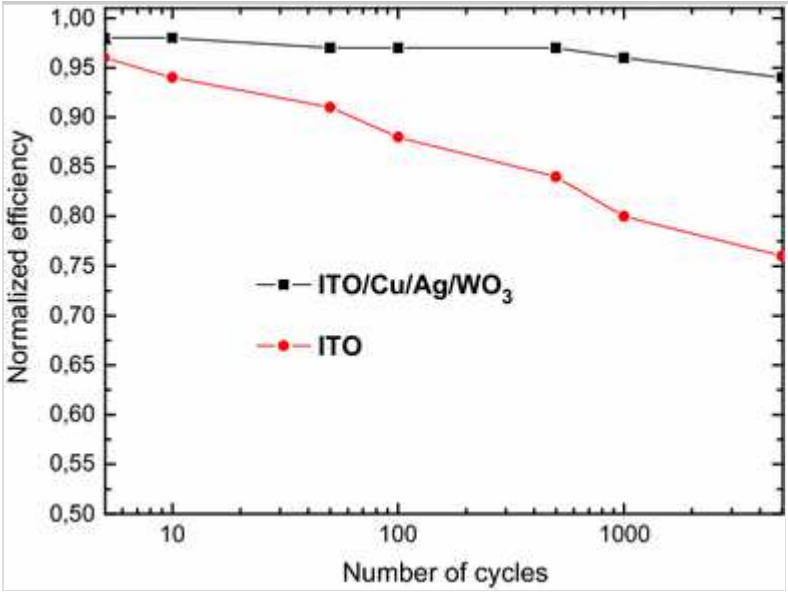

4. Conclusion

The present study allows us to show concretely that the sheet resistance of the electrodes can be an important issue when the active surface area of the photovoltaic cells is increased. This issue is important in the case of flexible substrate due to the fact that the nature of the substrate (plastic) limits the post-annealing temperature which makes the conductivity lower than that of films deposited on glass. In the present work, we have shown that this issue can be addressed by covering the ITO by a bilayer of Metal, Cu/Ag and finally by a layer of a transition metal oxide, MoO_3 or WO_3. The structures obtained exhibit a smaller sheet resistance while preserving for the most part its transmission qualities. The study of the organic solar cells shows that the best power conversion efficiencies are obtained using ITO/Cu/Ag/WO_3 structures.

Acknowledgments

The authors would like to thanks CNRST (PPR/2015/9) Ministère, Morocco) for funding support.

References

1. M.C. Scharber, N.S. Sariciftci, Prog. Polym. Sci. **38**, 1929–1940 (2013)

2. N. Leclerc, P. Chávez, O.A. Ibraikulov, T. Heiser, P. Lévêque, Polymers **8**, 11 (2016). doi:10.3390/polym8010011

3. R. Meerheim, C. Körner, B. Oesen, K. Leo, Appl. Phys. Lett. **108**, 103302 (2016)

4. Z. He, B. Xiao, F. Liu, H. Wu, Y.L. Yang, S. Xiao, C. Wang, T.P. Russel, Y. Cao, Nat. Photon. **9**, 174–179 (2015)

5. J.C. Bernède, J. Chil. Chem. Soc. **53**, 1549–1564 (2008)

6. M. Aleksandrova, Adv. Mater. Sci. Eng. (2016). doi:10.1155/2016/4081697

7. Y. Mouchaal, G. Louarn, A. Khelil, M. Morsli, N. Stephant, A. Bou, T. Abachi, L. Cattin, M. Makha, P. Torchio, J.C. Bernède, Vacuum **111**, 32–41 (2015)

8. Xue et al., ACS Appl. Mater. Interfaces **6**, 16403–16408 (2014)

9. H.M. Stec, R.A. Hatton, ACS Appl. Mater. Interfaces **4**, 6013–6020 (2012)

10. L. Cattin, Y. Lare, M. Makha, M. Fleury, F. Chandezon, T. Abachi, M. Morsli, K. Napo, M. Addou, J.C. Bernède, Sol. Energy Mater. Sol. Cells **117**, 103–109 (2013)

11. G. Haacke, J. Appl. Phys. **47**, 4086–4089 (1976)

12. L. Barkat, M. Hssein, Z. ElJouad, L. Cattin, G. Louarn, N. Stephant, A. Khelil, M. Ghamnia, M. Addou, M. Morsli, J.C. Bernède, Phys. Sol. A Stat. (2016). doi:10.1002/pssa.201600433
AQ3

13. L. Cattin, F. Dahou, Y. Lare, M. Morsli, R. Tricot, K. Jondo, A. Khelil, K. Napo, J.C. Bernède, J. Appl. Phys. **105**, 034507 (2009)

14. S.-W. Cho, J.-A. Jeong, J.-H. Bae, J.-M. Moon, K.-H. Choi, S.W. Jeong, N.-J. Park, J.-J. Kim, S.H. Lee, J.-W. Kang, M.-S. Yi, H.-K. Kim, Thin Solid Films **516**, 7881–7885 (2008)

15. I. Pérez Lopéz, L. Cattin, D.-T. Nguyen, M. Morsli, J.C. Bernède, Thin Solid Films **520**, 6419–6423 (2012)

16. W. Greenbank, L. Hirsch, G. Wantz, S. Chambon, Appl. Phys. Lett. **107**, 263301 (2015)

17. T. Winkler, H. Schmidt, H. Flügge, F. Nikolayzik, I. Baumann, S. Schmale, T. Weimann, P. Hinze, H.-H. Johannes, T. Rabe, S. Hamwi, T. Riedl, W. Kowalsky, Org. Electron. **12**, 1612–1618 (2011)